Science of Sintering, **46** (2014) 365-375

doi: 10.2298/SOS1403365L

UDK 549.514; 622.785

Influence of Nitrogen and Air Atmosphere During Thermal Treatment on Micro and Nano Sized Powders and Sintered TiO_2 Specimens

N. Labus[1*)], S. Mentus[2,3], Z. Z. Đurić[1], M. V. Nikolić[4]

[1]Institute of Technical Sciences of SASA, Knez Mihailova 35, 11000 Beograd, Serbia
[2]Faculty of Physical Chemistry, Studenski trg 12-16, 11158 Belgrade, University of Belgrade, Serbia
[3]Serbian Academy of Sciences and Arts, Knez Mihailova 35, 11000 Belgrade, Serbia
[4]Institute for Multidisciplinary Research, University of Belgrade, Kneza Viseslava 1, 11000 Beograd, Serbia

Abstract:

The influence of air and nitrogen atmosphere during heating on TiO_2 nano and micro sized powders as well as sintered polycrystalline specimens was analyzed. Sintering of TiO_2 nano and micro powders in air atmosphere was monitored in a dilatometer. Non compacted nano and micro powders were analyzed separately in air and nitrogen atmospheres during heating using thermo gravimetric (TG) and differential thermal analysis (DTA). The anatase to rutile phase transition temperature interval is influenced by the powder particle size and atmosphere change. At lower temperatures for nano TiO_2 powder a second order phase transition was detected by both thermal techniques. Polycrystalline specimens obtained by sintering from nano powders were reheated in the dilatometer in nitrogen and air atmosphere, and their shrinkage is found to be different. Powder particle size influence, as well as the air and nitrogen atmosphere influence was discussed.

Keywords: *Sintering, Nanopowder, Dilatometry, TG/DTA*

1. Introduction

Recent interest in TiO_2 is due to its wide band gap semiconductor properties and easily modulating surface properties. During irradiation with ultraviolet light with a wavelength energy larger than the band gap energy catalytic chemical activity at the surface is noted [1]. Changing band gap energy and surface structure promises enlargement of the number of possible light wavelengths that can be used in catalytic purposes [2].

Phase transition in TiO_2 is mostly concerned and described with usual modifications of differently oriented and attached structural TiO_6 octahedral units. The usually encountered transformation is anatase to rutile phase, where the latter represents the most stable modification. Both, the anatase and the rutile phases have been thoroughly studied. This phase transition is regarded as a reconstructive one where four rutile octahedral units are mutually attached with two coinciding edges, while the anatase structure consists of four attached edges. The anatase – rutile phase transition shows complex kinetics with separated nucleation

*) **Corresponding author**: nebojsa.labus@itn.sanu.ac.rs

and growth processes. Since diffusion is guided by two mechanisms, one with oxygen vacancies movement and the second with titanium interstitial defects relaxation, the process can be described as cooperative movements of oxygen and titanium atoms. According to this, concentrations of oxygen vacancies and interstitials are highly influential on the phase transformation process. Stress and atmosphere favors different mechanisms in a different way [3].

When air and nitrogen atmosphere interchanges are concerned, the pressure of the gases surrounding the bulk specimen can be considered as a comparatively small change on the pressure scale usually observed and has an influence only if the observed oxide is nonstoichiometric [4]. Such a small pressure change can become significant if the particular induced point defects concentration is rising with the observed particular state function increase [5,6]. Concentration increase of certain point defects ultimately can lead to a phase transition [7,8]. Namely a single crystallographic shear plane [9] known as the Wadsley defect [10], when increased in number induces the appearance of Magnelli phases, Ti_nO_{2n-1}[11]. The first phase in this homology group is Ti_2O_3 and it is morphologically considered an added row on the bulk surface [12]. This phase shows the second order phase transition frequently observed by the change in conductance [13]. The origin of this change is basically described as band gap lowering due to electronic excitations and electron states degeneration at the end of the temperature phase change interval. This phase transition is also observable as a heat capacity rate change, since changes in electron transition states induce changes in lattice parameters as well [14].

Diffusion in bulk and consequently at the reacting surface occurs in TiO_2 using two mechanisms: Ti interstitials with a dangling bond mechanism and oxygen vacancies mechanism through bridging oxygen atoms [12]. Oxygen anion substitution with nitrogen can be used since it is more effective in an experimental setup [15]. Calculations aimed at predictions of expected properties have indicated the same possibility [16]. Besides these induced substitution point defects, oxygen vacancies are the influential reactant evolving during heating. The strain influence on vacancies is extremely interesting as vacancy diffusion can be governed with residual micro strain through bulk as an entity and also through the lattice [17]. Besides their formation and their behavior during diffusion, surface interaction of vacancies with atmosphere ingredients is commonly observed [18].

Regardless to the before mentioned complexity of titanium as an oxide, different starting specimens as powders and bulk polycrystalline specimens during heating in different atmospheres show different behavior and microstructure. In this work the observed changes during heating in different atmospheres that produced the final microstructures are all used for the possible deduction and explanation of the underlying processes.

2. Experimental

The TiO_2 powders used were in two forms. TiO_2, nanopowder, Alfa Aesar 99.7% anatase with sizes of particles from 10 to 15 nm and sub micro powder Aldrich TiO_2 Titanim IV oxide Anatase [1317-70-0] 99.8% CAS 232033-500G. Thermogravimetric (TG) and differential thermal analysis (DTA) of sample powders in Pt pans, in the temperature interval from room temperature up to 1200°C, in both nitrogen and air atmospheres, was carried out simultaneously using the SDT 2960 thermobalance TA instrument. The heating rate was 15°C/min, while the gas flow rate was 70 cm^3s^{-1}.

TiO_2, nanopowder Alfa Aesar, and sub micro Aldrich TiO_2 powder were compacted with 200 MPa without a binder and lubricant uniaxally by double sided action compaction. Dilatation for the sintering process, first batch, first run, was recorded in air atmosphere on the compacted specimen with a heating rate of 10°C/min up to 1400°C with 5 minutes isothermal holding time and cooling recorded with declaratively - 20°C/min cooling rate, on a

Bähr Geratebau 802s dilatometer. Sintered specimens from the first batch, first run, were discarded regarding further heating experiments and the obtained results are only presented as dilatation and shrinkage rate.

Sintering was also performed on a second batch as a first run, but now up to 1100°C in a Lenton tubular furnace in air atmosphere. The heating program schedule was 10°C/min up to 1100°C, isothermal holding 60 minutes at 1100°C, with a cooling rate -25°C to 400°C. These sintered second batch samples were then reheated in the dilatometer, second run, at a 10°/min heating rate to 1100°C, with isothermal holding of 20 minutes and cooling to 400°C with –10°C/min. The two atmospheres were used during the second run. The flow rate was 1.1 cm^3s^{-1} for both air and nitrogen atmospheres. Specimens for the nitrogen atmosphere dilatation recording were cleaned by evacuating the chamber up to 60 Pa vacuum, and then purged with nitrogen, repeating the procedure twice. After cleaning, nitrogen was induced with a regulated flow and the measuring dilatation recording mode was entered when the temperature program was started.

Scanning electron microscopy was performed on a Vega Tescan TS 5130MM device. Specimens were broken and the breakage was performed at room temperature. Micrographs were recorded for specimens sintered from nano powder in air atmosphere, first batch, first run, and for the reheated sintered specimens in air and nitrogen atmospheres, second batch, second run.

3. Results and discussion

Measured DTA and TGA diagrams for TiO_2 nano and micro powders are shown in fig.1. Shrinkage and shrinkage rate of the TiO_2 nano and micro powders during heating in air are shown in fig.2.

The weight loss shown in fig.1. for TiO_2 micro powders is approximately below 0.5% while for the nano powder it is 7%. Desorption processes for the nano powder are measurable and completed up to 110°C as shown in fig.1. The DTA diagram at 500°C shows that the heat capacity is changing from a growth trend to reduction of its value. The temperature range where the anatase to rutile phase transition occurs, starts from 600°C and ends at above 1000°C, respectively [3]. For both powder particle sizes, fig.1, the anatase to rutile change onset is shifted to higher temperatures for nitrogen atmosphere. Although, the phase transition onset has changed due to the atmosphere influence, this phase transition is known to be crystallite size dependent. Similar thermal intervals detected in DTA for the micro powder are 930°C to 1020°C for nitrogen and 880°C to 990°C in air are observed also for the nano powder, 700°C to 810°C in nitrogen atmosphere and 730°C to 820°C in air atmosphere. These intervals presumably represent some energy consuming nucleation processes but since they are not detected on the shrinkage rate diagram given in fig.2, these processes cannot be interpreted surely but only as an energy consuming nucleation process. Final exothermic peaks are shifted with changes in particles size to higher temperatures, micro powder 1005°C for nitrogen and 1010°C for air and the nano powder 1130°C and 1135°C. For these exothermic events the influence of atmosphere shows only a 5°C difference.

During sintering in the dilatometer the anatase to rutile phase transition is detected in air atmosphere for the nano and micro powder, as shown in fig.2. Recognizable changes detected as the anatase to rutile phase transition process interruption during sintering for the nano powder are from 903°C to 1153°C as shrinkage rate are indicated on fig.3, while for the micro powder 1045°C to 1173°C, fig.2. The onset and completion of the anatase to rutile phase transition for the nano powder are limited with irregular but overall constant shrinkage rate intervals. Presumably the nucleation process and grain impingement are different for the anatase to rutile phase transition when powder particle sizes are changed.

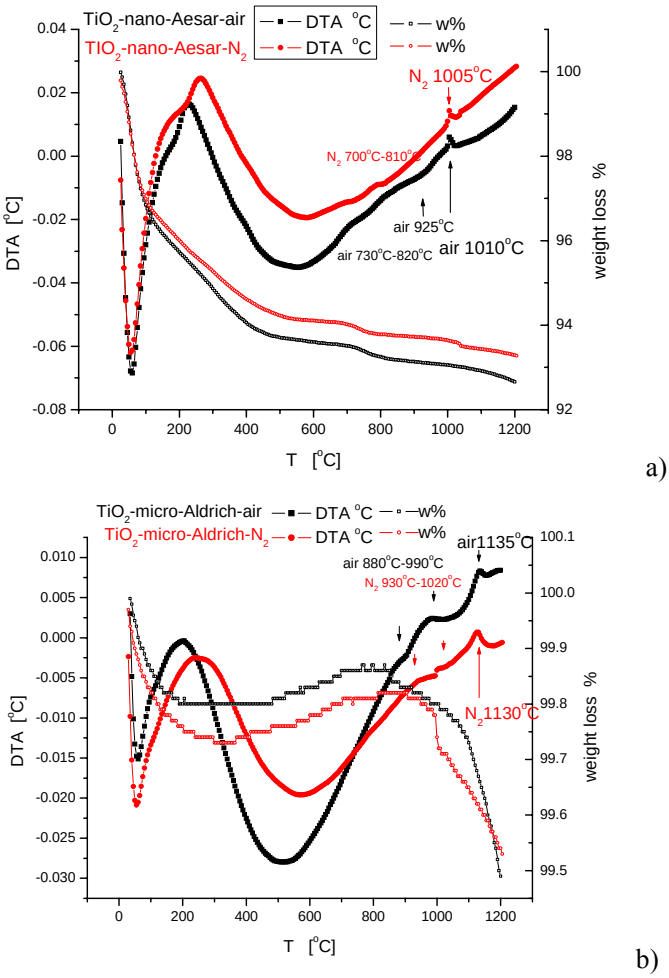

Fig. 1. DTA of powders and TGA function of the a) TiO_2 nano and b) TiO_2 micro powders in nitrogen and air atmosphere.

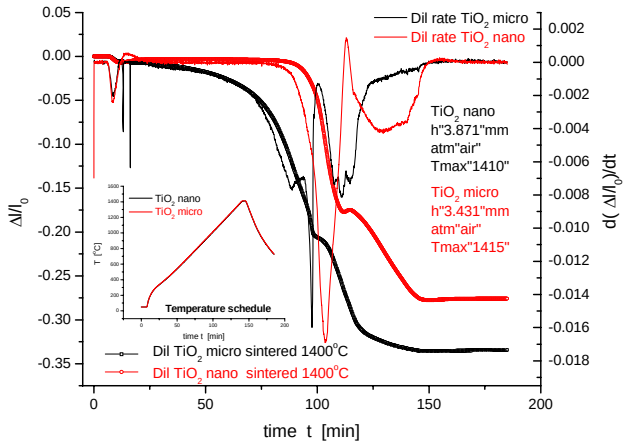

Fig. 2. Dilatation and dilatation rate of the sintering process for nano TiO_2 and micro TiO_2 compact: the temperature schedule is shown in the inset.

The sintering process is also influenced by powder particle size [19]. The nano particle onset differs from the value determined for the compact made from micro powder since particle rearranging is present. Also recrystallization and subsequent grain growth processes are separated for nano powder [20].

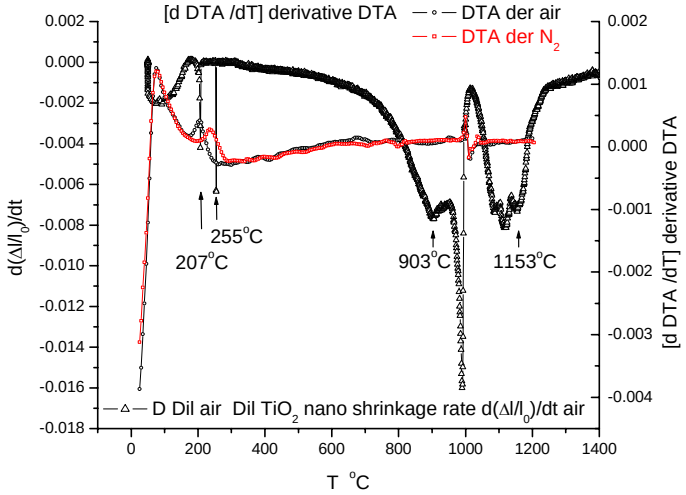

Fig. 3. Shrinkage rate as a function of temperature and DTA derivative in regard to temperature for TiO_2 nano powders in air and nitrogen atmospheres.

The shrinkage rate of TiO_2 nanopowder shown on fig.3. is the same derivative from the dilatation presented on fig.2. On the DTA diagram for the nano powder recorded in air on fig.1.a) at 925°C can be linked with the onset of shrinkage changes at 903°C. The most intensive event for both thermal techniques is sharply at the same temperature at 990°C.

Fig.3. also shows the first derivative of the DTA signal obtained for the TiO_2 nano powder in air and nitrogen atmospheres. It is not so often that the first derivative of the DTA signal is pointed, but the experimental and calculated specific heat anomaly is treated in this way [14]. The atmosphere influence on that transition is from 175°C to 260°C in air atmosphere and 195°C to 290°C in nitrogen, which is a 20°C shift induced by atmosphere change. This shift is pronounced on fig.3. for the first derivative of DTA in different atmospheres. This shift existing on DTA derivative diagrams on fig.3. should be regarded as a specific heat capacitance change originating from its electronic part, and is considered as a second order phase transition [13]. The suggested second order phase transition can be subscribed to Ti_2O_3 phase existence and it is not clearly observable for the micro powder.

In fig.3. the shrinkage rate for the nano powder compact shows two sudden events. The first one is at 207°C and the second one is at 255°C. With the heating rate of 10°C/min the first event is taking place in the 202°C to 213°C interval with 36 seconds duration, while the second one is occurring even faster in the 253°C to 255°C interval in only 14 seconds. These dilatometric shrinkage rate peaks are well superimposed on the DTA derivative on the same picture for air atmosphere. These changes can be also ascribed to the existence of a Ti_2O_3 phase. Namely, Ti_2O_3 is expected in the high strained nano powder particle surface due to structural rearrangement of this stoichiometry [1]. They can originate from relaxation processes of nano powder particles. Relaxation processes are divided into normal surface relaxation, where surface atoms are finding their equilibrium positions, and relaxation where shear strain relaxations are leading to rearranging atoms at the surface, sort of "flattening" the surface of the particle due to disappearing of low angle strains that is known as tangential relaxation [21].

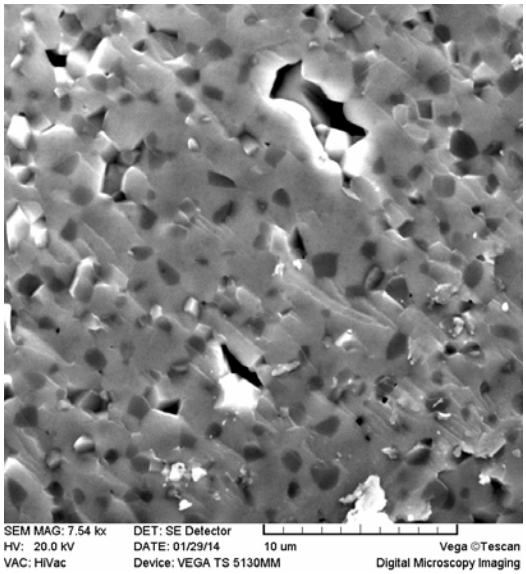

Fig. 4. Scanning electron micrograph of the TiO_2 nano powder, sintered at 1100^{o}C 1 h air atmosphere.

Nano powder sintering performed in the first heating process presented on fig. 2, and the shrinkage rate shown on fig. 3. involves sintering mechanisms that are entirely different to micro powders. In the case of micro powders when fast heating is applied, the starting stage of sintering with neck formation entraps interparticle pores [22]. Afterwards during recrystallization, when once pinned out from the grain boundary, pores are becoming rounded in shape and as thermodynamically stable are very hard to eliminate. Opposite to this, nano powders during sintering reduce the specific surface area by particle rearrangement, where interparticle pores are so small that they can be compared to grain boundary thickness. Such a dimensional ratio leads to pores disappearing during the enormous amount of shrinkage explained by pore coalescence followed by the mechanism of pore extrusion enabled by oxygen vacancy diffusion [23]. Shrinkage through recrystallization forms small grains, leading to nanocrystallinity. Recrystallization is competing here with the occurrence of pores collected from coalescence but not extruded by oxygen vacancies diffusion. So, the microstructure shown in fig.4 should not be compared by the grain sizes, but with respect to the closed porosity noticed on the breakage. The micrograph on fig.4. represents a sintered specimen with large and small pores. Large pores can be open or closed according to the whole bulk specimen. They show an irregular shape and undefined depth for the scanning electron microscopy. Small pores, on the other hand, are typical representatives of closed porosity. Breakage was done at room temperature and represents an intergranular cleavage fracture although, the micrograph shown in fig.4. is without recognizable grain boundaries. The starting powder had a declared 10 to 15 nm particle size, which is relatively small on the sintering powders scale where a nano domain is calculated to be from 10 to 100 nm. The recrystallization process, in that case, is extremely fast since the powder particle's core represents irregularities for the nucleation process. The grain impingement phenomenon is according to this sudden and grains are initially small and undistinguished. In the TiO_2 sintered compact, pore coalescence and oxygen vacancy diffusion mechanism in this stage is the main mechanism. So, the observed closed porosity is made by sudden nucleation and grain growth competing with a large amount of oxygen vacancies that cannot be extruded elsewhere but form closed pores inside the yet non defined grain structure. This is easily readable from the dilatation sintering shrinkage rate diagram presented on fig. 2. and fig. 3, as well as from the microstructure of the sintered specimen in air atmosphere shown in fig. 4.

Thus, although with rounded sides, still with the polygonal shape recognizable, closed pores are numerous and as such they are hindering typical grain impingement during recrystallization and remain on the grain triple junctions.

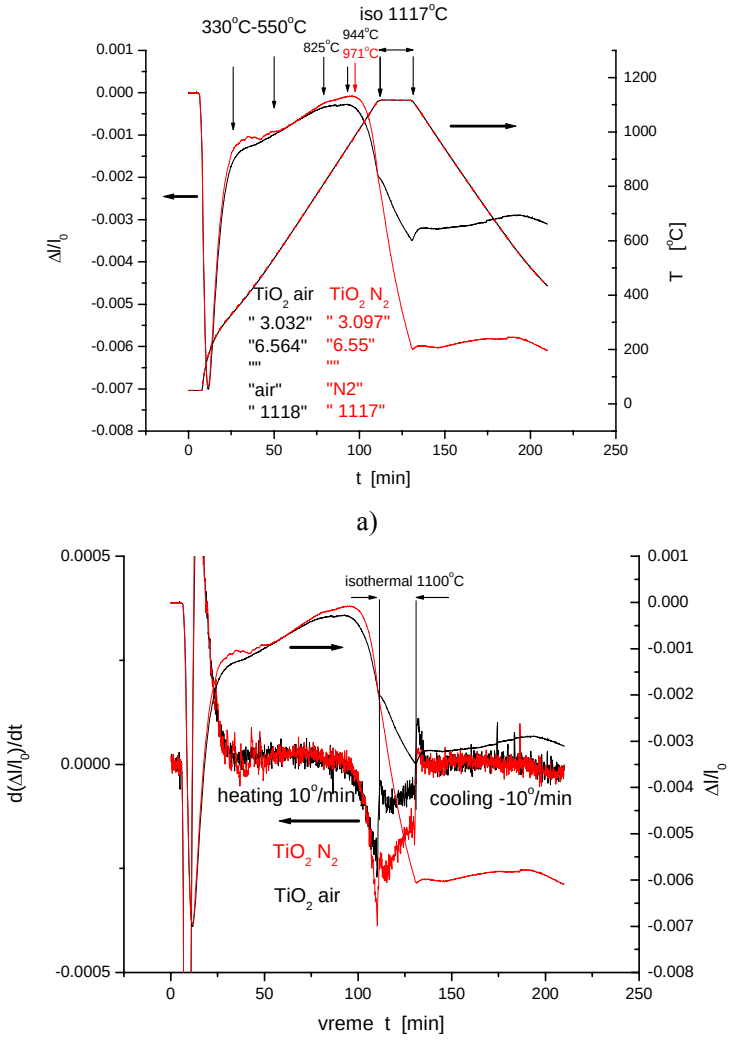

Fig. 5. Dilatation and temperature of nano TiO_2 during the reheating a) and shrinkage rate b) as a function of time in two different atmospheres, air and nitrogen, of the previously sintered specimen at 1100°C.

During reheating the sintered specimen is expected to be prone to atmosphere influence due to its unstable structure with closed porosity and high diffusion paths on grain boundaries as shown in fig. 4. Fig. 5. shows two previously sintered specimens of TiO_2 reheated in the dilatometric furnace, and dilatation was monitored in two different atmospheres, air and nitrogen. Distinct temperature intervals emphasized on fig.5. can be further discussed. The first temperature interval between 330°C and 550°C shows the difference in dilatation of TiO_2 due to atmosphere influence. Nitrogen atmosphere is showing discontinuity in dilatation, which can be either discontinuity or nitrogen introduction irregularity. The start of expansion to shrinkage interchange is at different temperatures. A higher shrinkage rate is also observed at the end of the non-isothermal period, but for nitrogen

atmosphere, fig. 5.b). The third temperature interval is isothermal holding period at 1117°C in duration of 20 minutes. The declared maximal temperature on the data sheet presented on fig. 5.a) is only one degree difference so the comparison can be correctly deduced. During the non-isothermal to isothermal heating change in schedule, an increasing number of vacancies become constant. Here, the change in shrinkage rate, fig. 5.b), is sudden and simultaneous. It is also noticeable that shrinkage rates during isothermal holding are different. The rate of shrinkage is falling faster in nitrogen than in oxygen atmosphere during isothermal holding, fig. 5.b). This is also visible on fig. 5. as greater maximal shrinkage of the specimen in nitrogen atmosphere. It is always pronounced as a period of shrinkage rate change needed for the equilibrium establishment with constant increase of the shrinkage rate [24]. The same influence during cooling, but now from diminishing the concentration of oxygen vacancies, as well as different atmospheres influence, is kinetically observable at the onset of the temperature schedule for the beginning of cooling.

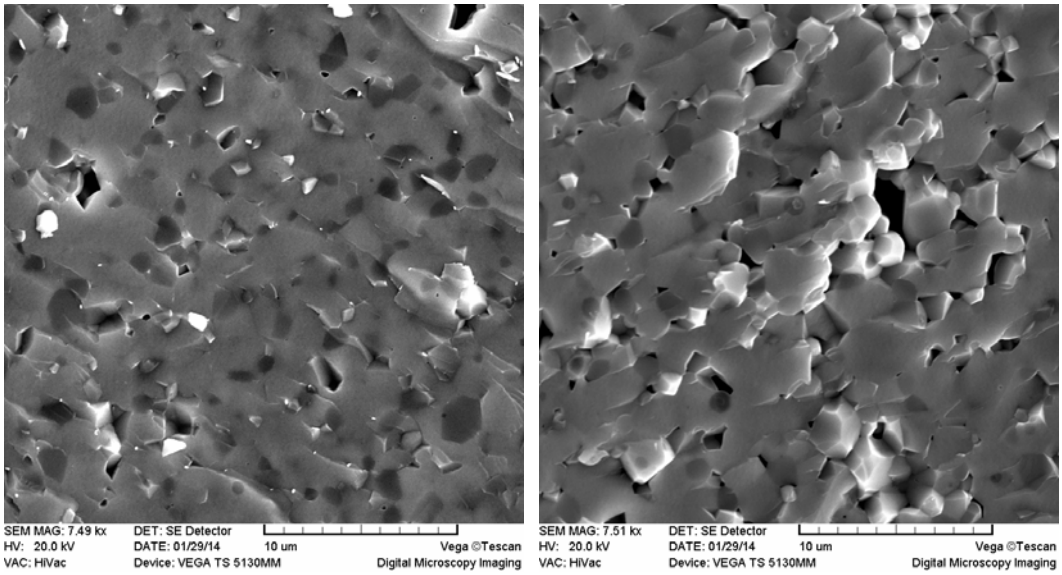

a) b)

N_2 air

Fig. 6. Scanning electron micrograph of TiO_2 nanopowder previously sintered and then a) reheated 1100°C 20 minutes, nitrogen atmosphere, b) reheated 1100°C 20 minutes, air atmosphere.

The second run of heating changed the microstructure in a different manner fig.6.a) for air and fig.6.b) for nitrogen atmosphere. Namely, in nitrogen atmosphere the microstructure retained closed porosity, although pores are larger and more randomly distributed through the bulk specimen, yet their shape is still polygonal in the presented section of micrographic view obtained also by breakage. Opposite to this, the second heating cycle in air atmosphere, fig.6.b) results in a lower number of closed pores and their shape becomes more rounded, while the dimensions of visible closed pores did not change.

Explanation of the atmosphere influence change on the microstructure lies in the fact that diffusion of the vacancies is faster than atomic species and their annihilation with oxygen present in air atmosphere is leading to closed porosity disappearance. The difference between micro and nano powder sintered compacts is that in micro powders [25,26] closed pores are from different origin. Closed porosity in nanopowders does not originate from inter powder particles pores as in micro powders, but from collected vacancies. As such, during further heating they behave as regular closed pores and in air atmosphere attaining their well

recognizable circular shape. In air atmosphere, as well, they reduce in number due to oxygen vacancies recombination through high diffusion paths, fig.6.b). If the source of recombination is hindered by the atmosphere change to nitrogen, fig.6.a), closed pores retain their polygonal shape, formed by stitching between the grain boundaries, unable to relax inside the uniform crystal structure by unpinning with grain boundary migration, or diminish in number by the high diffusion paths oxygen vacancies recombination.

4. Conclusion

The expected powder particles size change shifts the anatase to rutile phase transition for approximately 200^{o}C in nitrogen atmosphere and in air only 150^{o}C, favoring always the nano sized powder. This phase transition regarding micro or nano powder separately is influenced by atmosphere. For micro powder the air atmosphere lowers the temperatures of the onset and finish of the transition for rudely 40^{o}C, while for the nano powder air atmosphere compared with nitrogen rises temperatures for about 20^{o}C. The final exothermic peak above 1000^{o}C is 125^{o}C lowe for the nano powder, while the atmosphere influence lowers it for only 5^{o}C in nitrogen atmosphere. Dilatometric differences for nano and micro powders sintered in air are reflected in shifting towards higher temperatures in the case of the micro powder. A second order phase transition for nano powder in air is determined by both thermal techniques to be in the interval from 207^{o}C to 255^{o}C, and shifts in nitrogen atmosphere for 20^{o}C to higher temperatures. Polycrystalline specimens in nitrogen atmosphere are showing larger shrinkage resulting from a higher shrinkage rate after a late onset, followed by intensive isothermal shrinkage. Micrographs made for sintered nano powder in air and for reheated sinter made from nano powder in different atmospheres, show that closed porosity is significantly reduced by reheating, especially by reheating in air atmosphere.

Acknowledgement

The authors would like to express their gratitude to Jugoslav Krstić and Miodrag Zdujić for useful advice. This work was supported by the Ministry for Science, Education and Technological Development of the Republic of Serbia, projects OI172057 and III45014.

5. References

1. U. Diebold, Structure and properties of TiO_2 surfaces: a brief review, Appl.Phys. A, 76, 681-687 (2003).
2. K. I. Hadjiivanov, Dmitar G. Klissurski, Surface Chemistry of Titania (Anatase) and Titania Supported Catalysis, Chemical Society Review, 1996, 25, 61-69.
3. А.С: Бережной, Многокомпонентные системы оксилов, Изд.Наукова думка, Киев, 1970. стр.77.
4. R. Dieckman, Point defects and transport in non-stoichiometric oxides: solved and unsolved problems, J.Phys.Chem.Solids, Vol. 59, No.4. pp.507-525, 1998.
5. M. Ozawa, Effect of oxygen release on the sintering of fine CeO_2 powder at low temperature, Scripta Materialia, 50 (2004) 61-64.
6. R. Dieckmann, "Cobaltous Oxide Point Defect Structure and Non-Stoichiometry, Electrical Conductivity, Cobalt Tracer Diffusion." Zeitschrift Für Physikalische Chemie 107, no. 2 (January 1977): 189–210.

7. S. Iijima, J. G. Allpress. "High Resolution Electron Microscopy of $TiO_2 \cdot 7Nb_2O_5$." Journal of Solid State Chemistry, 7, no. 1 (May 1973): 94–105.
8. H.-I. Yoo, J.-H. Lee, M. Martin, J. Janek, H.Schmalzried, Experimental evidence of the interference between ionic and electronic flows in an oxide with prevailing electronic conduction, Solid State Ionics, 67 (1994) 317-322.
9. A. D. Wadsley, "Mixed Oxides of Titanium and Niobium. II. The Crystal Structures of the Dimorphic Forms $Ti_2Nb_{10}O_{29}$." Acta Crystallographica 14, no. 6 (June 1, 1961): 664–670.
10. A. D. Wadsley, S. Andersson, in Perspectives in Structural chemistry, J. D. Dunitz and J. Albers (Eds), Wiley, New York (1970), Vol.III, pp.1-58.
11. A. A. Gusev, E. G. Avvakumov, A. Zh. Medvedev, A. I. Masliy, Ceramic Electrodes Based on Magneli Phases of Titanium oxide, Sci. Sint., 39 (2007) 51-57.
12. U. Diebold, The surface science of titanium oxide, Surface Science Reports, 48 (2003) 53-229.
13. C.N.R. Rao, K.J. Rao, Phase transitions in Solids, Mc Graw Hill, 1978, p.75.
14. J.M. Honig, Some aspects of electrical properties of metal oxides, Deffects nad transport in oxides (Eds) Martin Seltzer, Robert I. Jaffee, 1974, Plenum press, New York, pp. 315-330.
15. R. Asahi, T. Morikawa, T. Ohwaki, K. Aoki, Y Taga, Visible Light Photocatalyst in nitorgen Doped Titanium Oxides, Scinece vol 293, 13 July 2001.269-271.
16. C. di Valentin, G. Pacchioni, A. Selloni, Origin of the different photoactivity of N doped anatase and rutile TiO_2, Physical Review B 70, 085116 (2004).
17. Z.-W. Wang, D.-J. Shu, M. Wang, N.-B. Ming, Diffusion of oxygen vacancies on a strained rutile TiO_2 (110) surface, Physical Review B, 82, 165309 (2010).
18. M. A. Anderson, W. S. Epling, et.al, Interaction of Molecular Oxygen with Vacuum-Annealed TiO_2 (110) Surface, Molecular and Dissociative Channels, J.Phys.Chem, B 1999, 103, 5328-5338.
19. В. И. Новиков, Л.И.Трусов, В.Н.Лапавок, Т.П.Гелеишвили, Особенности процессов переноса массы при спекании ультрадисперсных порошков, Порошковая металлургия, 1983, Но.7, с.39-46.
20. Y. Suyama, A. Kato, Sintering of fine TiO_2 powders prepared by Vapor - phase reaction, J.Ceram.Soc.Jap., 89 [3] 1981, 140-147.
21. И. П. Арсентьева, М. М. Ристић, Ультрадисперсные металличееские порошки: получение, структура, спекание, Белград, Центр за мультидисциплинарного обучениа Белгградского Университета, Институт технических наук сербской академий наук и искустов, 1987. стр.78.
22. C. Nivot, F.Valdeviso, P. Goeuriot, Nitrogen Pressure Effects on Nonisothermal Alumina Sintering, Journal of European Ceramic Society, 26, (2006), 9-15.
23. В. И. Новиков, Л. И.Трусов, В. Н. Лапавок, Т. П. Гелеишвили, О механизме низкотемпературной дифузии, активированной мигрирующей границей, Физика твредого тела, том 25, в. 12, 1983, с.3696-98.
24. P.Roura, J.Costa, J.Farjas, Is sintering enhanced under non-isothermal conditions?, Materials Science and Engineering, A337, (2002), 248-253.
25. S. Stevanovic, V. Zeljkovic, N. Obradovic, N. Labus, Investigation of Sintering Kinetics of ZnO by Observing, Reduction of the Specific Surface Area, Science of Sintering, 39 (2007) 259-265.
26. N. Labus, J. Krstić, S. Marković, D. Vasiljević-Radović, M V. Nikolić, V. Pavlović, $ZnTiO_3$ Ceramic Nanopowder Microstructure Changes During Compaction, Science of Sintering, 45 (2013) 209-221.

Садржај: *Испитиван је утицај атмосфере ваздуха и азота током загревања TiO_2 прахова нано и микро величине честица као и синтерованих поликристалних узорака. Синтеровање нано и микро прахова у атмосфери ваздуха праћено је дилатометријски. Прахови који претходно нису пресовани нано и микро величина честица, анализирани су методом термогравиметрије ТГ и диферницијалне термијске анализе ДТА у атмосфери ваздуха и азота. Температурски интервал фазног прелаза из анатаса у рутил је претрпео промене услед различите величине честица као и услед утицаја атмосфере. На нижим температурама код нано праха уочен је фазни прелаз другог реда коришћењем обе термалне технике. Поликристални узорци добијени синтеровањем нано праха у ваздуху загервани су поново у атмосферама азота и ваздуха и њихово скупљање је различито. Утицај величине честица праха као и утицај атмосфере азота или ваздуха је коментарисан.*

Кључне речи: *синтеровање, нано прахови, дилатометрија, ТГ/ДТА*